

1 Estimating Biochemical Concentration in Food Using Untargeted

2 Metabolomics

Michael Sebek^{1,+}, Giulia Menichetti^{1,2,+,}
Albert-László Barabási^{1,2,3†}

⁵ ¹Network Science Institute and Department of Physics, Northeastern University, Boston, MA,
⁶ USA

⁷ ²Department of Medicine, Brigham and Women's Hospital, Harvard Medical School, Boston, MA,

8 USA
9 ³Department of Network and Data Science, Central European University, Budapest, Hungary
10 [†]These authors contributed equally to this work.

11 Abstract

Untargeted metabolomics can detect hundreds of biochemicals in food, yet without standards, it cannot quantify them. Here we show that we can take advantage of the universal scaling of nutrient concentrations to estimate the concentration of all biochemicals detected by untargeted metabolomics. We validate our method on 20 raw foods, finding an excellent agreement between the predicted and the experimentally observed concentrations.

[†]Corresponding author e-mail: barabasi@gmail.com

17 The documented impact of diet on health has prompted national efforts to catalogue
18 the biochemical composition of food¹, like the USDA Standard Reference² that reports the
19 concentration of 150 nutrients in 9,759 foods. The data was collected using gravimetry
20 (AOAC934.06), liquid chromatography (AOAC988.15), and fluorimetry (AOAC967.22), ex-
21 perimental methodologies that can detect and quantify the concentration of a biochemical
22 in food. Meanwhile untargeted metabolomics can detect hundreds more compounds within
23 a single experiment, but only relative concentration are inferred, mainly because of the
24 unknown fraction of molecules ionized for each compound^{3,4}. Targeted metabolomics cir-
25 cumvents ionization efficiency⁵ by using standard curves to determine the concentration, a
26 low-throughput procedure that eliminates the advantages of untargeted metabolomics over
27 established methodologies by increasing the time and cost over current AOAC methods.
28 Untargeted metabolomics needs to move beyond relative concentrations for adoption by
29 food composition catalogues. Here we report a method to predict concentrations from un-
30 targeted metabolomics, offering researchers a way to extend their results beyond relative
31 concentrations. This is advantageous for food composition catalogues which can leverage
32 the predictions to report expected concentrations and their potential variance for foods in a
33 high-throughput way.

34 We show that the universal scaling of nutrient concentrations across the food supply⁶
35 allows us to determine nutrient concentration in untargeted metabolomics. We performed
36 metabolomics experiments on 20 raw plant ingredients to minimize the influence of human
37 processing and span the phylogenetic tree as well as edible parts of plants (fruits, leaves,
38 roots) to get a representative diversity of plant composition across the food supply (SI Ex-
39 perimental Design). Focusing on the 295 biochemicals found in at least 10 ingredients, we
40 obtained their nutrient distribution across the food samples using the experimentally mea-
41 sured peak areas. In metabolomics, the peak area for each compound, n , in each food, f ,
42 measures only the ionized concentration, $c_{f,n}^{ionized}$. It is unknown what fraction of a com-
43 pound's total concentration becomes ionized, preventing peak area from directly measuring

44 the total concentration, $c_{f,n}$. The primary contributors to this loss in efficiency ($E_{f,n}$) are
45 sample preparation ($E_{f,n}^{prep}$), extraction protocols ($E_{f,n}^{ext}$), and ionizability ($E_{f,n}^{ion}$) such that
46 $E_{f,n} = E_{f,n}^{prep} \cdot E_{f,n}^{ext} \cdot E_{f,n}^{ion}$. Since our experiments used the same experimental protocol for
47 each food item, $c_{f,n}$ differs from $c_{f,n}^{ionized}$ by $E_{f,n}$ where only the food sample matrix provides
48 the largest deviations between measured peak areas across the foods for each compound.

49 To apply the universal scaling of nutrient concentration to the measured peak areas
50 in untargeted metabolomics, we need $c_{f,n}^{ionized}$ to follow the universal features of nutrient
51 concentration⁷: (i) constant standard deviation ($\langle s_n \rangle$), (ii) symmetric distribution, and (iii)
52 translational invariance. A universality rooted in the biochemical mechanisms responsible
53 for the synthesis and consumption of each compound within an organism. If it holds for
54 peak areas, this would mean that we can use the universality to find the total concentrations
55 from peak areas; however, $E_{f,n}$ can break the universality if it greatly varies between food.
56 Yet, we find that (i)-(iii) apply to the peak areas as well, with $\langle s_n \rangle = 1.41 \pm 0.50$. This
57 suggests that

$$E_{f,n} \approx \langle E_n \rangle \quad (1)$$

58 for each compound, where $\langle E_n \rangle$ is the mean efficiency across all foods, conserving the uni-
59 versality. We also find that the peak areas follow log-normal distributions similar to the
60 nutrient concentrations in [7] (SI Universal Scaling Law of Metabolomics). Lastly, we com-
61 pare the universal scaling observed for nutrients reported by the USDA (Fig 1a) with the
62 biochemicals obtained by our experiments (Fig 1b). We find that the linear standard devi-
63 ation of peak areas for a biochemical in MassSpec (σ_n^{MS}) relates to the mean peak area for
64 a biochemical in MassSpec (μ_n^{MS}) in the log-space via $\sigma_n^{MS} = e^{\alpha_{\sigma}^{MS}} (\mu_n^{MS})^{\beta_{\sigma}^{MS}}$, where α and
65 β are parameters of the power law fit, in excellent agreement with the USDA. These results
66 indicate that the efficiencies of the experiment ($E_{f,n}^{prep}$, $E_{f,n}^{ext}$, $E_{f,n}^{ion}$, etc.) are largely invariant
67 across food sample matrices.

68 Next, we test the correlations between the metabolomics variables (σ_n^{MS} , μ_n^{MS}) and their
69 respective counterparts of the USDA (σ_n^{US} , μ_n^{US}). Focusing on 19 foods and 31 biochemicals

70 reported in both datasets (SI USDA – Metabolomics Overlap), we find low correlation (R^2
 71 = 0.566), confirming that ionization efficiency obscures the relationship between the peak
 72 areas measured in MassSpec and the concentrations reported in the USDA via $\mu_n^{US} = \langle E_n \rangle$
 73 μ_n^{MS} . We can, however, estimate the concentration from peak area by leveraging (1) and the
 74 universal features (i)-(iii), followed by both metabolomics and USDA, indicating that the
 75 position of foods within the nutrient distributions between the datasets is largely conserved.
 76 For example, we can see that for pyridoxine (vitamin B6) the relative position of potato
 77 is the same in the metabolomics and the USDA distributions (Fig 1c). This suggests that
 78 we can use the distance between the individual food measurements and the median in the
 79 linear-space to connect the two distributions via

$$\frac{x_{(f,n)}^{US}}{e^{m_n^{US}}} \approx \frac{x_{(f,n)}^{MS}}{e^{m_n^{MS}}}, \quad (2)$$

80 where $x_{(f,n)}^{US}$ is the concentration of the biochemical for a food from the USDA, m_n^{US} is the
 81 mean log concentration of the nutrient in the USDA, $x_{(f,n)}^{MS}$ is the peak area of the biochemical
 82 in the food from experiments, and m_n^{MS} is the mean log peak area of the biochemical in the
 83 experiments (SI Proportionality Validation).

84 To assess the validity of (2) we curate 113 high-quality food-biochemical pairs in overlap
 85 between the two datasets by filtering to analytical values with at least 4 measurements (SI
 86 Curated Pairs), then estimate $x_{(f,n)}^{US}$ and compare to the reported value in the USDA by
 87 calculating prediction error,

$$error = \begin{cases} \frac{x_{(f,n)}^{est}}{x_{(f,n)}^{US}} & x_{(f,n)}^{US} < x_{(f,n)}^{est} \\ \frac{x_{(f,n)}^{US}}{x_{(f,n)}^{est}} & x_{(f,n)}^{US} \geq x_{(f,n)}^{est} \end{cases} \quad (3)$$

88 where $x_{(f,n)}^{est}$ is the estimated concentration as found by Equation (2), $x_{(f,n)}^{est} = \frac{x_{(f,n)}^{MS}}{e^{m_n^{MS}}} e^{m_n^{US}}$.
 89 When the estimated and reported concentrations are equal, the prediction error is 1.0 and so
 90 values closer to 1.0 is desirable. Using (3), we observe a 3.1 mean error and a 2.4 median error

91 for the $x_{(f,n)}^{est}$ values (Fig 2a, blue line) with 73% of the values below 4.0 error, an outcome
92 comparable with other untargeted metabolomics estimation methods⁸, which report a 2.0-
93 4.0 mean error. Importantly, this approach should work for any sample where biological and
94 volumetric constraints synergistically determine the concentration (SI Method Guidelines).

95 The methodology (2) requires the concentration m_n^{US} of the biochemicals, known only
96 for nutrients reported in the USDA. To overcome this limitation, we rely on the finding that
97 compound concentrations in bacterial and human cells are correlated with their chemical
98 properties of the compounds⁹, allowing us to infer m_n^{US} for nutrients not present in the USDA.
99 We created a XGBoost model to predict $x_{(f,n)}^{US}$, taking as input the chemical properties of
100 biochemicals (molecular weight, logP, logS, hydrogen bonding inventory, number of charged
101 atoms, non-polar surface area) and phylogenetic lineages of foods (class, order, family, genus
102 classifications). Leave-one-out validation of the trained model shows 70% of the $x_{(f,n)}^{US}$ values
103 within 2.0 error and 90% within 4.0 error of the true value ($R^2 = 0.931$, Fig 2b), confirming
104 the model is accurate (SI Gradient Boosting Methodology).

105 Using XGBoost to estimate m_n^{US} , (2) can estimate $x_{(f,n)}^{US}$ in individual foods using the
106 peak areas, observing a 3.4 mean error (Fig 2a, red line) and 73% of the values below a 4.0
107 error. XGBoost allows us to determine the concentration of biochemicals not reported in
108 the USDA, but detected in our experiments. For example, while S-allylcysteine in garlic is
109 not reported by USDA, our untargeted experiments allow us to estimate its concentration as
110 0.158 g/100g. Using FoodMine¹⁰, we found six published measurements for S-allylcysteine
111 in garlic, with an average at 0.115 g/100g, giving a 1.4 error, demonstrating the possibility
112 of using ML-models to extend the estimated concentrations from (2) beyond the USDA.
113 While promising, the accuracy and generalizability of such models require further study (SI
114 Beyond the USDA).

115 The proposed methodology offers actionable concentration estimates to complement the
116 standard presence/absence information delivered by untargeted metabolomics, helping man-
117 aging costs and resources of future studies. We find that our method estimates concentration

118 in untargeted metabolomics with a 3.1 mean error, relying on the universal features of nu-
119 trient distributions and offers comparable performance to the current structural similarity
120 method (4.3 mean error) without requiring chemical standards and ionization efficiency pre-
121 diction method (2.1 mean error) without needing rarely measured ionization efficiencies⁸.
122 Here, we rely on publicly available training data, facilitating the seamless integration of
123 our methodology in the decision-making process of health risk assessments, as seen with
124 established methods¹¹ considering food-borne compounds.

125 References

126 [1] European Food Information Resource. List of Food Composition Databases at EuroFIR.
127 https://www.eurofir.org/food-information/food-composition-databases (2009).

128 [2] U.S. Department of Agriculture & Agricultural Research Service. FoodData Central.
129 https://fdc.nal.usda.gov (2019).

130 [3] Purves, R.W., Gabryelski, W. & Li, L. Rapid Commun Mass Spectrom 12, 695–700
131 (1998).

132 [4] Müller, C., Schäfer, P., Störtzel, M., Vogt, S. & Weinmann, W. J. Chromatogr. B 773,
133 47–52 (2002).

134 [5] Ankney, J.A., Muneer, A. & Chen, X. Annu. Rev. Anal. Chem. 11, 49–77 (2018).

135 [6] Menichetti, G., Barabási, A-L., & Loscalzo, J. Annu. Rev. Nutr. (2024).

136 [7] Menichetti, G. & Barabási, A.-L. Nat. Food 3, 375-382 (2022).

137 [8] Kruve, A., Kiefer, K. & Hollender, J. Anal. Bioanal. Chem. 413, 1549–1559 (2021).

138 [9] Bar-Even, A., Noor, E., Flamholz, A., Buescher, J.M. & Milo, R. PLoS Comput. Biol.
139 7, (2011).

140 [10] Hooton, F., Menichetti, G. & Barabási, A.-L. Sci. Rep. 10, 16191 (2020).

141 [11] Groff, L.C., et al. Anal. Bioanal. Chem. 414, 4919–4933 (2022).

142 Acknowledgements

143 We thank Dr. Roger Giese and Dr. Pushkar M. Kulkarni at the Department of Pharmaceu-
144 tical Sciences, Northeastern University for preparing the food samples. Experiments were
145 performed by Metabolon Inc., led by Nino Esile, Dr. Brian Ingram, and Nathan Testa. This

¹⁴⁶ work was partially supported by NIH grant 1P01HL132825, American Heart Association
¹⁴⁷ grant 151708, ERC grant 810115-DYNASET, and Rockefeller Foundation grant 2019 FOD
¹⁴⁸ 026.

¹⁴⁹ **Data and Code Availability**

¹⁵⁰ The data and codes used to develop the methodology are openly available at our GitHub page
¹⁵¹ at <https://github.com/Barabasi-Lab/Quantifying-Uncertaged-Metabolomics>. The raw
¹⁵² metabolomics data for the study is available on Metabolights at <https://www.ebi.ac.uk/metabolights/MTBLS3319>.
¹⁵³

¹⁵⁴ **Author Contributions**

¹⁵⁵ A.L.B. and G.M. conceived the research. M.S. led the metabolomics experiments and per-
¹⁵⁶ formed the data analysis. A.L.B. and G.M. advised and guided the research. M.S. wrote the
¹⁵⁷ manuscript. A.L.B. and G.M. reviewed and edited the manuscript.

¹⁵⁸ **Competing interests**

¹⁵⁹ A.L.B. is a scientific founder of Scipher Medicine, Inc., which applies network medicine
¹⁶⁰ strategies to personalized drug selection, and Naring, Inc., which applies data science to
¹⁶¹ food and health. All other authors declare no competing interests.

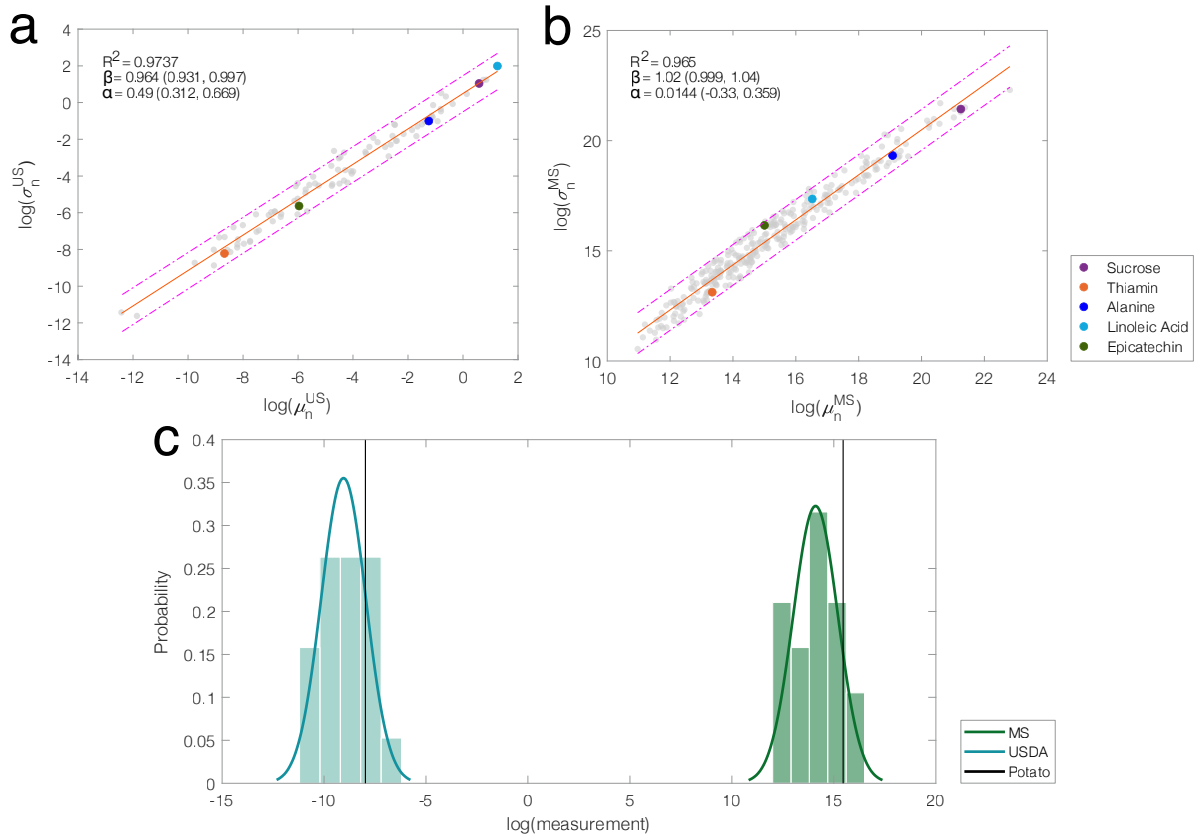


Figure 1: **Estimating Concentrations in Untargeted Metabolomics.** (a) Universal scaling law for nutrients within the USDA subset, relating the standard deviation, σ_n^{US} vertical axis, to the average nutrient concentration, μ_n^{US} horizontal axis, for 94 nutrients in 510 foods. Dashed lines are confidence intervals. Colored dots are compounds we selected to compare their relative positions between a) and b). (b) Universal scaling for our untargeted metabolomics experiments, relating the standard deviation, σ_n^{MS} , to the mean peak area, μ_n^{MS} , for 295 biochemicals in 20 foods. (c) Nutrient distributions using the 19 foods in overlap between the USDA and our experiments for pyridoxine: experiments (peak area, red) and USDA (g/100g, blue). The position of potato is shown in each distribution (black lines).

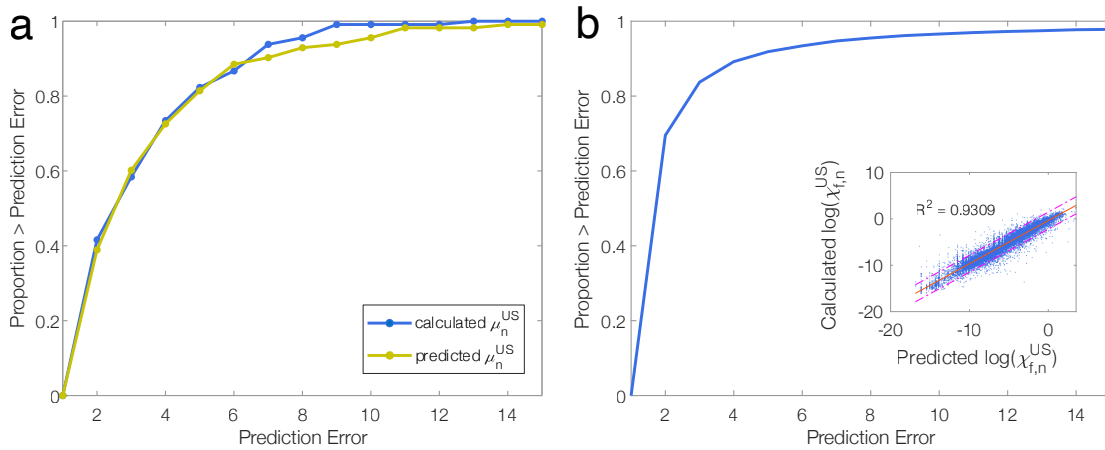


Figure 2: Prediction Error Curves. The proportion of estimated nutrient concentrations in individual food items below specified error values. **(a)** Error curve plots using the curated 113 biochemical-food pairs for the calculated μ_n^{US} from the USDA (blue) and predicted μ_n^{US} from a XGBoost model (yellow), taking as input the chemical properties of biochemicals (molecular weight, logP, logS, hydrogen bonding inventory, number of charged atoms, non-polar surface area) and phylogenetic lineages of foods (class, order, family, genus classifications). **(b)** Error curve of the Leave-one-out predicted concentrations for the 18,458 biochemical-food pairs in the training data. Inset: the relationship between calculated $x_{(f,n)}^{US}$ from the USDA and predicted $x_{(f,n)}^{US}$ from the XGBoost model. This shows that we can predict the concentrations reported in the USDA with a correlation of $R^2 = 0.931$ between the predicted and real concentrations.